

# PROCEEDINGS OF SPIE

[SPIDigitalLibrary.org/conference-proceedings-of-spie](https://spiedigitallibrary.org/conference-proceedings-of-spie)

## Slumped glass optics development with pressure assistance

Salmaso, B., Basso, S., Civitani, M., Ghigo, M., Hołyszko, J., et al.

B. Salmaso, S. Basso, M. Civitani, M. Ghigo, J. Hołyszko, D. Spiga, G. Vecchi, G. Pareschi, "Slumped glass optics development with pressure assistance," Proc. SPIE 9905, Space Telescopes and Instrumentation 2016: Ultraviolet to Gamma Ray, 990523 (19 July 2016); doi: 10.1117/12.2232273

**SPIE.**

Event: SPIE Astronomical Telescopes + Instrumentation, 2016, Edinburgh, United Kingdom

# Slumped Glass Optics development with pressure assistance

B. Salmaso<sup>1a</sup>, S. Basso<sup>a</sup>, M. Civitani<sup>a</sup>, M. Ghigo<sup>a</sup>, J. Hołyszko<sup>a</sup>,  
D. Spiga<sup>a</sup>, G. Vecchi<sup>a</sup>, G. Pareschi<sup>a</sup>

<sup>a</sup>INAF/Brera Astronomical Observatory, Via E. Bianchi 46, 23807 Merate, Italy

## ABSTRACT

Thin glass mirrors are a viable solution to build future X-ray telescopes with high angular resolution and large collecting area. This approach is very attractive for the optics implementation of future X-ray astronomy projects like the X-ray Surveyor Missions in USA, the XTP mission in China and the FORCE mission in Japan (all these projects could have an European participation). In the case of the X-ray Surveyor Mission, where a sub-arcsec angular resolution is requested, the use of actuators or post correction with sputtering deposition is envisaged. The hot slumping assisted by pressure is an innovative technology developed in our laboratories to replicate a mould figure. Our hot slumping process is based on thin substrates of Eagle XG glass to be thermally formed on Zerodur K20 moulds. This technology is coupled with an integration process able to damp low frequency errors. A continuous improvement in the reduction of the mid-frequency errors led to slumped glass foils with a potential angular resolution evaluated from the metrological data of a few arcsec. High frequency errors have been for a long time a critical point of our technology. In particular, the pressure assistance was leading to a partial replication of the mould micro-roughness, causing a non-negligible contribution to the Point Spread Function (PSF), in the incidence angle and X-ray energy range of operation. Therefore, we developed a new process to further reduce the micro-roughness of slumped glass foils, making now the technology attractive also for telescopes sensitive at higher X-ray energies. This paper provides the latest status of our research.

**Keywords:** hot slumping, thin glass mirrors, Zerodur K20, Eagle XG, X-ray segmented optics, Slumped Glass Optics

## 1. INTRODUCTION

Different astrophysical missions are considering thin glass foils as substrates for lightweight optics: X-ray Surveyor [1, 2, 3], XTP [4], FORCE [5]. Glass foils were also considered a viable alternative for the ATHENA mission [6]. The Brera Astronomical Observatory (INAF-OAB, Merate - Italy) has been working from 2009 till 2013 [7, 8, 9] to develop in Europe a Slumped Glass Optics (SGO) technology, alternative to the one based on silicon pores, and based on the slumping of thin glass foils. This activity has been initially carried out under ESA contract, in parallel to the work developed at NASA/GSFC and other institutes, and it is now being continued with other resources. Our SGO approach consists of a hot slumping technology to replicate the mould figure onto a thin glass substrate, with an integration process able to damp the low frequency errors of the slumped glass foils. An accurate description of our hot slumping and integration technologies can be found elsewhere [9, 10]. The process was developed for slumped glass foils with the following parameters: size of 200 mm x 200 mm, thickness of 0.4 mm and radius of curvature of 1 m, integrated in Wolter I configuration with a focal length of 20 m and an incidence angle of 0.7 deg.

Concerning the hot slumping technology, our innovation consists in the application of pressure to assist the replica of the mould figure during the thermal forming process (INAF patent TO2013A000687, 12 August 2013). A pressure of 50 g/cm<sup>2</sup> was experimentally demonstrated to be essential to minimize the mid frequency errors of the slumped foil [11]. We have now developed a model to support the importance of pressure in the hot slumping technology [12]. This model extends, with the application of pressure, an existing theoretical approach [13] developed to explain the corrugations experimentally observed in the glass foils slumped during the HEFT glass substrates fabrication at Columbia University.

During the past research, several prototypes (Proof Of Concepts, POCs) have been already produced (POCs #1-2-3-4) and tested in X-rays, showing a continuous improvement of the optical performances [11, 14]. Different materials for the

<sup>1</sup> bianca.salmaso@brera.inaf.it; phone +39-02-72320428; fax +39-02-72320601; [www.brera.inaf.it](http://www.brera.inaf.it)

glass and the mould were tested and the best results were found by using Corning Eagle XG for the glass and Schott Zerodur K20 for the mould [11]. The thermal cycle and the pressure value were tuned, cleaning protocols were implemented, the thermal gradients inside the slumping environment were reduced, and the process was optimized in order to avoid air bubble entrapping between the mould and the glass surface. The latter may occur when a K20 mould with high optical quality and smoothness is used in order to minimize the errors in the slumped glass foil [11], but this problem has been fixed. This research work led to a great improvement of the slumped glass quality both in terms of shape and roughness. In order to tune the slumping process parameters, some figures of merit were chosen and some assumptions were made in order to compute the expected angular resolution (Half Energy Width, HEW) after integration. In particular, based on Finite Element Analysis [15], a perfect correction of the azimuthal errors was assumed and no impact on the longitudinal correction was assumed from the azimuthal errors; the longitudinal profiles were damped with factors dependent on the harmonic components and the distances from the ribs; moreover no errors were assumed neither from the integration moulds, or the glue between the glass and the ribs. Based on these assumptions, we have computed with physical optics [16] the expected HEW values at 1 keV X-ray energy and 0.7 deg incidence angle, from longitudinal profiles taken on the slumped glass foils with the Long Trace Profilometer (LTP). The result is a simulated angular resolution improved from the initial 7 arcsec HEW to  $2.2 \pm 0.3$  arcsec in single reflection [17]. Some of the best glass foils produced with the recently developed process were integrated in the last prototype (POC#5). A discussion on the actual results obtained on this prototype is given in Section 5, while a more detailed analysis is reported elsewhere [18].

Some of our slumped glass foils were also used as substrates by the SAO-CfA group [3] to demonstrate the feasibility of the piezoelectric figure correction on cylindrical glass foils. We collaborate with SAO-CfA for the development of the mirrors of the X-ray Surveyor mission, that aims at an angular resolution  $< 1$  arcsec HEW, with an effective area 20 times larger than Chandra. To this end it is foreseen the use of piezoelectric elements on the back-side of the mirrors, in order to actively correct the profiles down to less than 1 arcsec. Actually the Eagle glass, differently from the D263 glass, used by NASA/GSFS, was shown to be compatible with the deposition process of the chosen piezoelectric material (PZT). In fact the PZT film, applied after the slumping process, requires a thermal cycle that reaches  $T = 550$  °C, and therefore requires substrates with annealing temperature considerably higher than the PZT ( $T_{\text{anneal-D263}} = 557$  °C,  $T_{\text{anneal-Eagle}} = 722$  °C). Active profiles corrections are also studied in Italy on our slumped Eagle glass foils [19]: the foils are integrated with glass ribs, after commercially available piezoelectric patches are glued on the back of the substrate. The piezoelectric elements are controlled with a tension signal carried by a printed circuit obtained by photolithography on the back side of the substrate. The concept of this research is to demonstrate the possibility to provide the correct voltage signal to the piezo elements from intra-focal measurements in X-rays.

Regarding the roughness, the pressure assistance was leading to a partial replication of the mould micro-roughness on the slumped glass foils, causing a non-negligible contribution from high-frequency errors to the PSF (depending on the incidence angle and photon energy), anyway keeping the contribution to the angular resolution (Half Energy Width, HEW) less than 1 arcsec at 1 keV, as computed for our configuration (radius of curvature of 1 m and focal length of 20 m). Several process improvements reduced the roughness from 21 to 11 Å (rms computed in the 5200-10 µm spatial wavelength). We have now developed a new slumping process that considerably reduces the high-frequency errors down to  $\sim 7$  Å in the same spectral band, without degrading the mid-frequency errors, making the technology attractive also for higher X-ray energies and higher incidence angles.

In this paper we present the results recently obtained in our hot slumping technology assisted by pressure. A pressure of 50 g/cm<sup>2</sup> was already experimentally demonstrated to be essential to minimize the mid frequency errors of the slumped foil [11]. Section 2 briefly presents the model we have developed to support the experimental result; the analytical description of the model can be found elsewhere [12]. Section 3 presents the results obtained in the last years. Section 3.1 summarizes the improvements in the slumped glass foils quality in terms of appropriate figures of merit. The research work was divided into six steps, where we have changed a few parameters or materials at a time; a detailed description of the process changes can be found in [17]. Section 3.2 presents the most recent result in terms of reduced roughness of the slumped glass foil, obtained by combining the 50 g/cm<sup>2</sup> pressure value (to reduce the amplitude of low- and mid-frequency errors) and a zero soaking time to reduce the mould roughness replication. Section 4 presents the expected angular resolution from the slumped glass foils at energies higher than 1 keV, and compares the results obtained with the previous and the more recent slumping process. Finally in Section 5, a comparison of the expected results and what experimentally obtained on the integrated glass foils is presented.

## 2. THE NEED OF PRESSURE: MODELLING AND EXPERIMENTS

During thermal slumping, if the glass and the mould get in contact, ripples in the glass surface can be formed, as consequence of the imperfect match of the two materials' CTEs. These ripples would relax in a time dependent, among others, on the glass viscosity: the relaxation time is longer at high viscosity. There are different models to describe relaxation in glasses. We have considered the model proposed in 2003 by Jimenez-Garate [13], as it simply describes the origin of the corrugations experimentally observed in our slumped glass foils, typically observed with spatial wavelength of 1-2 cm. We have developed a modification of the model [12], to account for the pressure exerted in our setup. We here summarize the result of this model, where we have computed the ripple relaxation time as:

$$\tau = \frac{\eta}{\frac{8S}{\lambda} + \frac{\rho g \lambda}{4} + \frac{P \lambda}{2h}} \quad (\text{Eq. 1})$$

where  $\eta$  is the viscosity,  $S$  is the surface tension of the glass,  $\lambda$  is the wavelength of the formed ripple,  $\rho$  is the glass density,  $g$  is the gravity acceleration,  $P$  is the applied pressure and  $h$  is the ripple height. Unlike the Jimenez-Garate model without pressure, the ripple relaxation time becomes dependent on the ripple height  $h$  and the applied pressure  $P$ . Eq. 1 shows that the application of pressure reduces the relaxation time.

In our process, a pressure of 50 g/cm<sup>2</sup> is applied just after the reaching of the maximum temperature  $T_{\text{soaking}}$ . In Figures 1 and 2 we compare the relaxation time at different temperatures, hence different viscosities. In Fig. 1, our soaking temperature is considered ( $T_{\text{soak}} = 750$  °C): during the 4 hours soaking time (blue line of Fig. 1-left), all ripples are relaxed, as shown by the absence of the interference fringes between the mould and the glass foil (Fig. 1-right): this is consistent with the prediction of the model (Fig. 1-left): all ripples with spatial wavelength of 1-2 cm are relaxed during the soaking time with the application of pressure (colored lines of Fig. 1-left), while they are not relaxed without the pressure application (black line of Fig. 1-left).

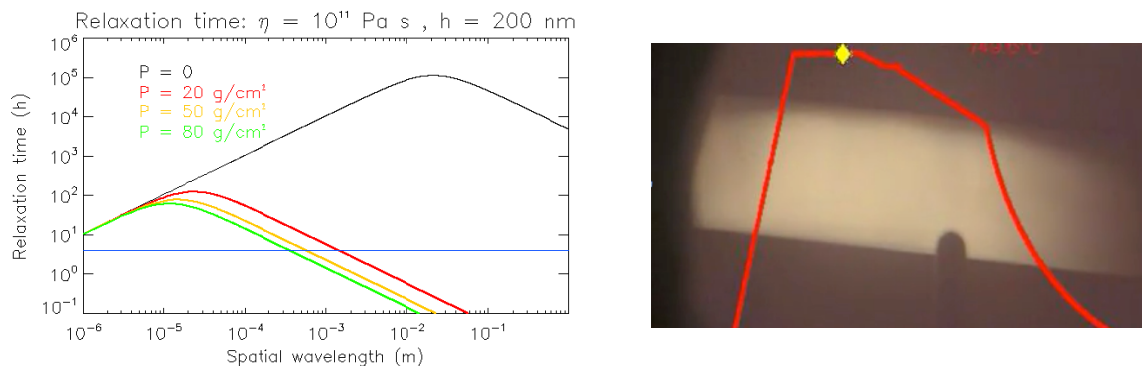


**Fig. 1** Relaxation of ripples for Eagle glass at the soaking temperature:  $T_{\text{soak}} = 750$  °C ,  $\eta_{\text{soak}} = 10^{11}$  Pas. Left: Predicted relaxation time of surface ripples versus ripple wavelength (ripple height of 200 nm are considered). The blue line corresponds to the soaking time of 4 h. Right: Image of the interference fringes between the glass and the mould, recorded during the slumping at the soaking temperature: all ripples are relaxed by the pressure, as shown by the absence of fringes.

In Fig. 2, the annealing temperature is considered ( $T_{\text{anneal}} = 722$  °C): ripples with spatial wavelength of 1-2 cm are not relaxed during the 2 hours soaking time (blue line of Fig. 2-left), also with the assistance of pressure. The criticality is also experimentally demonstrated by the reappearance of the interference fringes at a temperature just below the annealing. This justifies the use of very low cooling rate.

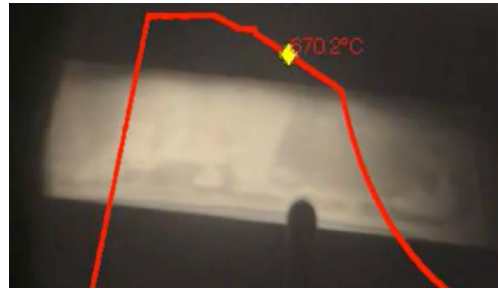
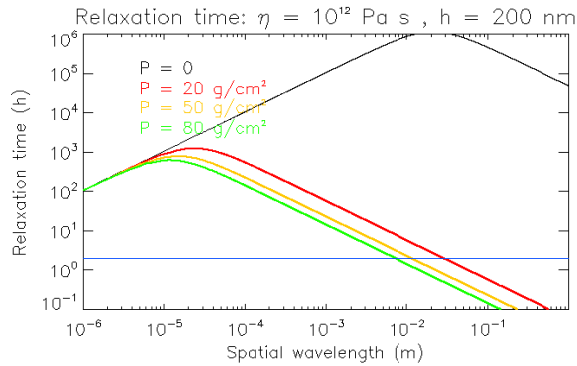


**Fig. 2** Relaxation of ripples for Eagle glass at the anneal temperature:  $T_{\text{anneal}} = 722 \text{ }^\circ\text{C}$ ,  $\eta_{\text{anneal}} = 10^{12}$  Pas. Left: Predicted relaxation time of surface ripples versus ripple wavelength (ripple height of 200 nm are considered). The blue line corresponds to the annealing time of 2 h. Right: Image of the interference fringes between the glass and the mould, recorded during the slumping just below the annealing temperature: the ripples reappearance is compatible with the criticality shown in Fig.2-left for the relaxation of ripples with 1-2 cm wavelength also with the presence of pressure.

### 3. RESULTS

#### 3.1 The improvement trend in our slumping process

Several modifications were implemented to optimize the slumping process. Since 2013, a total amount of about 100 glass foils were thermally slumped in order to improve the technology. For the ease of the interpretation, the research work was divided into six steps (Tab. 1): in each step, few parameters were modified as the thermal cycle, the pressure value, the thermal gradients inside the slumping environment, the mould height with respect to the glass foil, and the cleaning protocols [11]. While some of the experimental change of parameters determined real improvements, others did not really allowed us to obtain better results but, in any case, they helped us in achieving a better understanding and control of the process. Three different K20 moulds were used in carrying out this research [11]: one with poor surface quality (MK20-10), and two with higher surface quality (MK20-20 and MK20-20B), which considerably improved the slumped glass foils results in terms of mid- and high-frequency errors. Fig. 3 shows the mid-frequency improvement obtained on the K20 with higher surface quality.

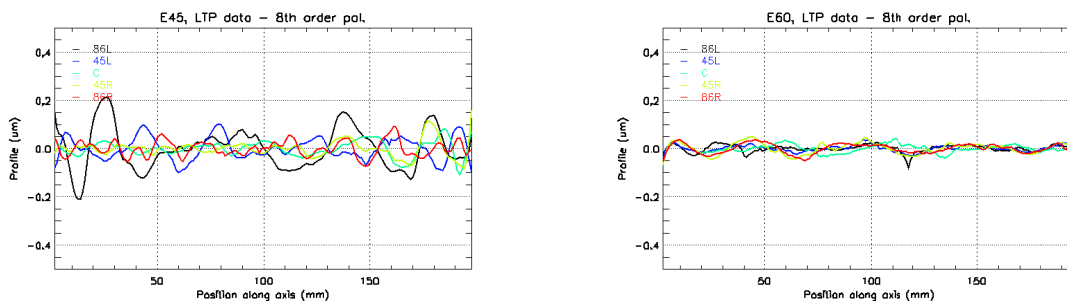


**Fig. 3** Mid-frequency content comparison of E45 (the best glass foil slumped on MK20-10) and E60 (the best glass foil slumped on MK20-20B). The graphs are obtained from raw LTP data after the subtraction of the best fit 8<sup>th</sup> order polynomial. They show the great reduction of mid-frequency errors by slumping of the mould with better quality surface.

Table 1 reports the result of the best glass foil for each of the six experiments (“steps”), as compared to a reference glass (code F18), a Schott AF32 glass foil, slumped on MK20-10 with the same parameters of the glass foils integrated into the POC#2 prototype.

The glass foils are compared in terms of:

- PV of the central LTP longitudinal scan, which is the less corrected during our integration procedure with ribs [11, 20];

- the expected HEW value computed in single reflection, from the longitudinal LTP profiles, at 1 keV and 0.7 deg incidence angle (named “as slumped”): this gives an indication of the mould replication in the low-frequency range;
- the expected HEW value computed in single reflection, from the longitudinal LTP profiles, at 1 keV and 0.7 deg incidence angle, after the simplified simulation of a perfect integration with six ribs: this is more sensitive to the glass quality in terms of mid-frequency errors, as the low frequency errors are damped during the integration according to the model [15];
- the rms of the micro-roughness as measured with a WYKO TOPO-2D interferometer in the spatial wavelength range [2640-10  $\mu\text{m}$ ]. This parameter is important to evaluate the worsening of the PSF due to the X-ray scattering up to 1 keV.

In Table 1, the results obtained for 10 glass foils slumped with the same process parameters are also reported (step 5), in order to evaluate the process stability. The result shows that the forming process is now stable, since the HEW value predicted after the simulation of the integration gives the same result within 0.3 arcsec, for an average value of 2.2 arcsec. This oscillation is mostly related to the error profiles with frequencies in the centimeter range. It should be noted that the low frequency errors have an impact just for the simulated HEW of the mirrors “as slumped” (i.e. without accounting for the corrections introduced with the integration), with a spread of 3.6 arcsec, for an average value of 18.7 arcsec.

In step 6, a new slumping process was developed to reduce the mould roughness replication: this is discussed in Section 3.2.

**Table 1:** Improvements of the most important parameters, which measure the quality of the slumped glass foils: peak to valley of the central LTP scan, expected HEW value from the raw LTP data (as-slumped), expected HEW value from LTP data after the simulation of a perfect integration, rms roughness from WYKO data. About 100 foils were slumped from 2013 till today: the results are divided into six steps, each one characterized by the improvement of some particular parameters; for each step the best glass results are presented. Step 5 reports the result of 10 glass foils slumped with the same process to present the process stability.

Step	Glass and mould description	Notes	Code of the best produced glass sample	PV of central scan [ $\mu\text{m}$ ]	Expected HEW [arcsec] @ 1 keV and 0.7 deg inc. angle		Micro-roughness rms [ $\text{\AA}$ ] [2640-10 $\mu\text{m}$ ]
					As slumped	Predicted after a simplified perfect integration	
0	AF32 on MK20-10	Reference glass: same parameters used for the glass integrated onto the POC#2 prototype	F18	17.6	120	6.8	20.8
1	AF32 on MK20-10	Mould height change, soaking time increase	F30	9.8	43.3	6.6	18.3
2	Eagle on MK20-10	Glass type change	E5	5.0	25.3	5.3	18.3
3	Eagle on MK20-20	Smoother mould	E21	9.0	40	3.6	12.8
4	Eagle on MK20-10	Mould height change, thermal gradients reduction, cooling rate reduction	E45	2.7	21.3	4.1	14.9
5	Eagle on MK20-20B	Process stability on smoother mould	10 glasses	$3.5 \pm 0.6$	$18.7 \pm 3.6$	$2.2 \pm 0.3$	$10.7 \pm 1.4$
6	Eagle on MK20-20B	NEW process for lower roughness substrates	E65	2.5	25.7	2.4	6.7

The data presented in Table 1 are plotted in Fig. 4, and compared with the requirement, as defined in [17].

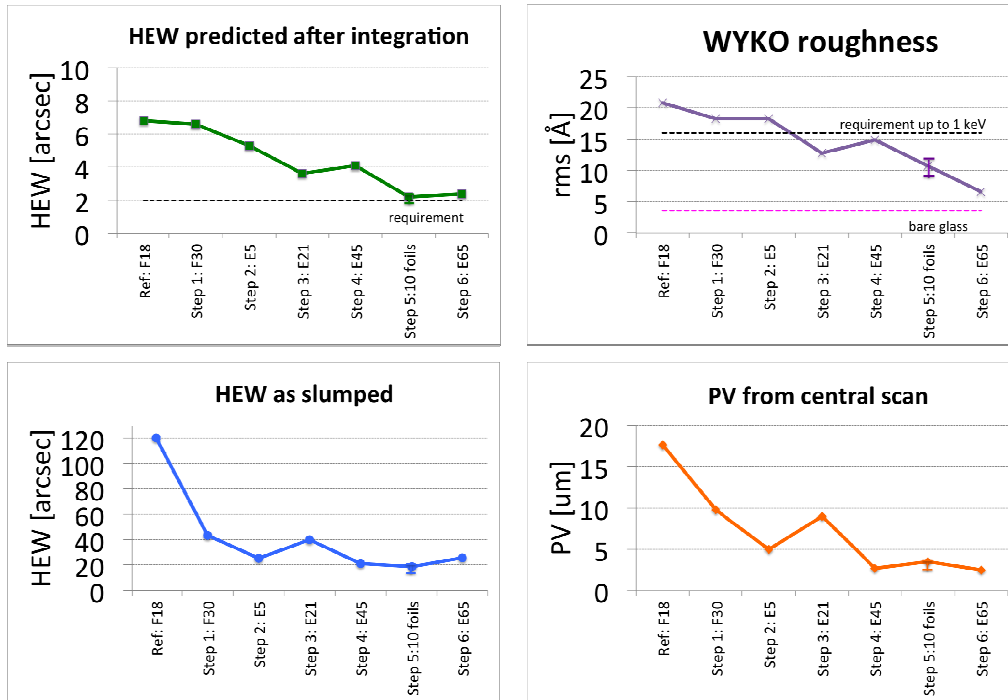


**Fig. 4** Trend of the key parameters selected to trace the process improvement (data of Table 1). Top left: HEW values expected from the LTP slumped glass profiles, obtained with physical optics [Raimondi, Spiga, D 2015] in single reflection after the simulation of a perfect integration; 2 arcsec were allocated for the profiles. Top right: Roughness from the WYKO data: slumped foils with roughness values  $< 16 \text{ \AA}$  would contribute with less than 1 arcsec at 1 keV to the final PSF. Bottom left: HEW computed from raw LTP data. Bottom right: PV of the central scan, the most critical as the less corrected during the integration. The error bar obtained from the 10 glass foils of step 5 has been also added.

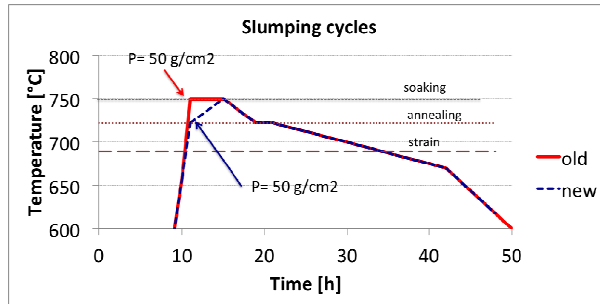
### 3.2 Results: the roughness reduction of step 6

The pressure assistance, although essential to reduce the errors contribution in the centimeter spatial wavelength range, was leading to a partial replication of the mould micro-roughness [11, 21]. Attempts to reduce the roughness replication, by reducing the pressure value below our standard value of  $50 \text{ g/cm}^2$ , were always leading to an increase in the mid-frequency errors [11].

In order to tackle this problem, we have developed a new slumping process (step 6) that reduces the mould roughness replication. This is obtained with the following process changes:

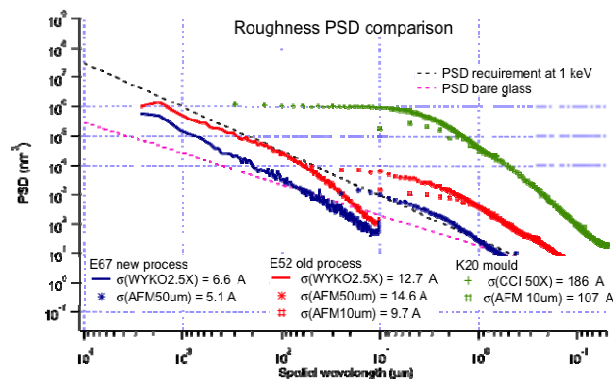
- 1) reduce to zero the soaking time, where the glass experiences the maximum temperature and therefore replicate at most the mould roughness,
- 2) decrease the heating rate to thermalize the mould and the glass foils at the highest temperature,
- 3) anticipate the pressure application time from the soaking to a temperature slightly higher than the annealing temperature, to avoid air bubble entrapping between the mould and the glass.

Fig. 5 compares the old and new thermal cycles.



**Fig. 5** Thermal cycles comparison: the blue dashed line represents the new thermal cycle that reduce the mould roughness replication (step 6 of Table 1). The red solid line represents the old thermal cycle of step 5 of Table 1.

Three glass foils were slumped with the new slumping process and they confirmed the obtained result. Fig. 6 shows the PSD due to micro-roughness, measured with a WYKO TOPO-2D and a stand-alone Veeco Explorer™ AFM, for one of the glass foils slumped with the new process (glass code E67, blue line), compared to one slumped with the old process (glass code E52, red line), in the spatial wavelength range from 2500 to 0.05  $\mu\text{m}$ . The micro-roughness is reduced in all the spatial wavelength range, while the contribution from the mid frequency errors is substantially unchanged, owing the pressure value of 50  $\text{g}/\text{cm}^2$  in both cases: in fact, the expected HEW computed from the LTP longitudinal, after the simulation of an ideal integration with 6 ribs, is 2.8 and 2.5 arcsec for E52 and E67, respectively. Fig. 6 reports also the K20 mould roughness for comparison.



**Fig. 6** PSD from roughness data for one glass foil slumped with the new process (glass code E67, blue line), and one slumped with the old process (glass code E52, red line). The K20 mould roughness (green line) is reported for comparison.

#### 4. EXPECTED HEW FROM PROFILE AND ROUGHNESS DATA

In order to evaluate the expected HEW values, we use the physical optics approach applied to X-ray mirrors [16], that is able to treat at the same time slope errors and diffuse scattering, coming from profile errors in a very broad range of spatial frequencies. The errors, as measured in the five LTP longitudinal profiles, results to be damped thanks to our integration method; the HEW values have been inferred considering a perfect simplified integration with six ribs [10, 9], and the roughness is considered by retrieving one of the possible profiles from the PSD analysis.

We have fully characterized the roughness of the E67 slumped glass foil. The PSD discrepancy of the WYKO and AFM roughness data, visible in Fig.6, was solved by the measurement with our Micro Finish Topographer (MFT), a phase shift interferometer equipped with several interferometric objectives which returns 2D maps. The measurements obtained with the 10X objective smoothly combine the WYKO and the AFM data (Fig. 7). The PSD obtained by these three instruments, combined with the LTP profiles damped with our simulated integration, were used to compute the expected HEW value.

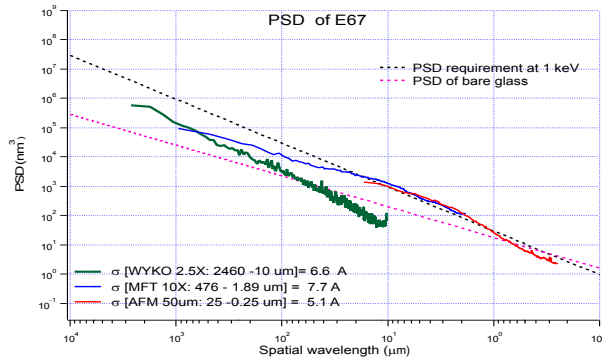


**Fig. 7** PSD from roughness data for the glass foil slumped with the new process (glass code E67). The glass was characterized with the WYKO TOPO-2D, the MFT interferometer and the AFM.

In Fig. 8, we compare the HEW values expected from a glass foil slumped with the new process (E67 glass code, blue line) with one slumped with the old process (E52 glass code, red line). Finally, also the HEW values computed from the profile data of the E67 glass foil and the roughness measured from the bare new glass foils are compared (pink line): this would give a lower limit to the roughness contribution to the final HEW. All HEW values are computed in single reflection, for incidence angle of 0.7 deg and focal length of 20 m, which are the technical parameters used for our prototypes up to now.

Fig. 8-left shows that the expected HEW value increases quite rapidly with increasing energy for the E52 glass foil (red line), the one slumped with the old process and with higher roughness value. The situation is much improved for the E67 glass foil (blue line), slumped with the new process and with a roughness halved in the WYKO range and reduced to 1/3 in the AFM range. The HEW value for the E67 glass foil increases from 2.5 to 6 arcsec, going from 1 to 6 keV, whereas a hypothetical slumped glass foil with the same profile errors of the E67 one, but roughness value as good as a brand-new glass, would go from 2.5 to 3.3 arcsec (pink line). Note that if the same HEW values are computed within a detector area of 26 mm<sup>2</sup> (actually 52 mm<sup>2</sup> were considered, due to the single reflection, Fig. 8-right), as the one of the PIXI detector at PANTER-MPE (Garching, Germany) the increase would be lower, going, for the E67 glass foils, from 2.5 @ 1 keV to 4.4 @ 6 keV arcsec: this is due to the fact that the scattering is largely distributed outside the detector area.

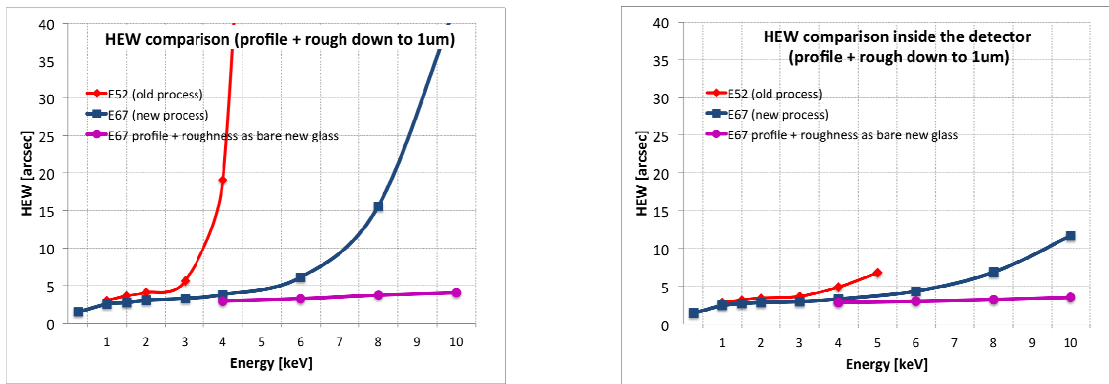


**Fig. 8** Expected HEW values computed from physical optics in single reflection, for 0.7 deg incidence angle and 20 m focal length. The LTP profiles after the simulation of a perfect integration with 6 ribs and one of the possible profiles obtained from the PSD data are considered for a glass foil slumped with the new process (E67, blue line), for a glass slumped with the old process (E52, red line) and for a hypothetical glass foil slumped with the same profile errors of the E67 one, but with no roughness degradation (pink line). Left: the expected HEW values. Right: the expected HEW values measured within a detector with size of 26 mm<sup>2</sup>, as the PIXI at PANTER.

To further improve the roughness of the slumped glass foils, a polishing process for the Zerodur K20 slumping mould should be defined, to reduce the roughness mould from 130 to 70 Å, as suggested by the result obtained from our best slumped glass with a roughness rms of 7 Å compared to the 3.6 Å of the brand-new bare glasses. This seems to be possible, as reported by Zeiss on a forming mould in Zerodur K20 developed for the hot slumping process by NASA: Schott prepared the forming mould [22], and Zeiss performed the polishing on the Wolter-I surface [23], reporting a mould surface roughness of 5-8 nm rms, as measured with the Promap 512.

## 5. COMPARISON OF THE PREDICTED HEW VALUES AFTER SIMULATED AND REAL INTEGRATION

Few glass foils from the Step 5 group were integrated into a new prototype, the POC#5 [18]. A brief comparison of the simulated and experimental data is given in this Section, while a more detailed discussion can be found in [18].

The POC#5 is composed of 4 layers; after the integration of all layers, the external one was measured with the Characterization Universal Profilometer (CUP) available in our laboratories [24], and about 12 arcsec HEW was expected from these data in double reflection. The LTP characterization of the external glass foils, after the simulation of a perfect integration, returned about 2.5 arcsec HEW in single reflection and about 5 arcsec in double reflection. To compare the two results, we can consider the following errors contribution:

$$HEW_{CUP-real-int} = \sqrt{HEW_{LTP-ideal-int}^2 + HEW_{int-mould}^2 + HEW_{other}^2} \quad (\text{Eq. 2})$$

In Eq. 2 we have split the 12 arcsec HEW, expected from CUP data after the real integration, into 5 arcsec expected from LTP data after ideal integration, 8 arcsec of contribution from the integration moulds [Civitani2014], and 7 arcsec that can be due to either integration errors, or the glue effects, or a too simplified simulation of the integration (considering for instance no contributions to the final HEW value from the azimuthal errors).

X-ray measurements of the POC#5 were obtained very recently at the PANTER-MPE facility, with a result of about 30 arcsec [18]. We plan to repeat the metrology analysis of the prototype to check for possible degradation of the optics, and therefore understand the worsening of the result compared to the expectation.

## 6. CONCLUSIONS

In this paper we have presented the continuous improvement of our hot slumping technology assisted by pressure for the production of thin glass mirrors for future X-ray missions. Our technology was developed for the IXO 20 m focal length configuration: 200 mm x 200 mm glass foils with thickness of 0.4 mm are produced with cylindrical shape and Radius of Curvature of 1 m by the hot slumping technology, and are then integrated in the Wolter-I configuration by freezing the Wolter shape with integration ribs. Figures of merit were chosen to demonstrate the trend of the optical quality of the substrates: a potential angular resolution in single reflection of about 2 arcsec HEW is reached, evaluated from metrological data at 1 keV X-ray energy and 0.7 deg incidence angle, after the simulation of a perfect integration of our cylindrical slumped glass foils onto the Wolter-I configuration. Actually this number is still very distant from what obtained after the real integration: this is partly due to the integration mould errors, which we plan to correct with Ion Beam Figuring. There is also a contribution from the glue, from the integration in general and possibly from using an over-simplified integration model, which assumes no effects from the azimuthal errors. The full analysis of the last integrated prototype, once returned from the X-ray PANTER facility, will be crucial for this understanding.

For what concerns the quality of the glass foils before the integration, the assistance of pressure to the slumping process has already been demonstrated to be crucial for the reaching of a good optical quality, especially to decrease the longitudinal profile errors in the centimeter range spatial wavelength. We have now introduced a model to support the use of pressure in our hot slumping technology: this extends a pre-existing model, which accounts for ripples creation in the slumped glass foil, with the introduction of the pressure. From the experimental point of view, a drawback of the use of pressure has been, for a long time, a too large replication of the mould micro-roughness: the high frequency errors of

our slumped glass foils were introducing a contribution to the final PSF of less than 1 arcsec at 1 keV, but a larger contribution was expected at higher energies. We have now developed a slumping process that reduce the high frequency errors, while keeping the quality already reached in terms of mid frequency errors by the use of a pressure value of 50 g/cm<sup>2</sup>. This makes our technology now attractive for X-ray energies higher than 1 keV: the roughness contribution to the final PSF is now estimated to be within 3.5 arcsec at 6 keV. To further improve this result, the Zerodur K20 surface should be polished to lower roughness, which was shown to be possible as reported by Zeiss on a slumping mould in K20 polished for NASA.

## ACKNOWLEDGMENTS

We kindly thank Thorsten Doehring for useful information on the Zerodur K20. All the group from SAO-CfA is acknowledged for their collaboration and profitable meetings and discussions.

## REFERENCES

- [1] Reid, P.B., Allured, R., Cotroneo, V., Hertz, E., Marquez, V., McMuldloch, S., Ben-Ami, S., Schwartz, D.A., Vikhlinin, A.A., Trolrier-McKinstry, S., Wallace, M.L., Jackson, T.N., Tananbaum, H.D., "*Development of 0.5 arcsecond adjustable x-ray optics: status update*," Proc SPIE 9905, this conference (2016)
- [2] Cotroneo, V., Allured, R., Reid, P.B., Vikhlinin, A.A., Pareschi, G., Civitani, M.M., Salmaso, B., "*Thermal forming of glass substrates for X-ray Surveyor optics*," Proc SPIE 9905, this conference (2016)
- [3] Allured, R., Hertz, E., Marquez, V., Cotroneo, V., Wallace, M.L., Salmaso, B., Civitani, M.M., Trolrier-McKinstry, S., Vikhlinin, A.A., Pareschi, G., Reid, P.B., "*Laboratory demonstration of the piezoelectric figure correction of a cylindrical slumped glass optic*," Proc SPIE 9905, this conference (2016)
- [4] Wang, Z., Shen, Z., Mu, B., Wang, X., Yang, X., Jiang, L., Qi, R., Wen, M., Zhang, Z., Ma, B., "*Development of the x-ray timing and polarization telescope optics*," Proc. SPIE 9144, 91441E (2014)
- [5] [https://files.aas.org/head2015\\_workshop/HEAD\\_2015\\_Hironori\\_Matsumoto.pdf](https://files.aas.org/head2015_workshop/HEAD_2015_Hironori_Matsumoto.pdf)
- [6] Basso, S., Civitani, M., Pareschi, G., Buratti, E., Eder, J., Friedrich, P., Furmetz, M., "*A design study of mirror modules and an assembly based on the slumped glass for an Athena-like optics*," Proc. SPIE 9603, 96030N (2015)
- [7] Proserpio, L., Ghigo, M., Basso, S., Conconi, P., Citterio, O., Civitani, M., Negri, R., Pagano, G., Pareschi, G., Salmaso, B., Spiga, D., Tagliaferri, G., Tintori, M., Terzi, L., Zambra, A. "*Production of the IXO glass segmented mirrors by hot slumping with pressure assistance: tests and results*," Proc. SPIE 8147, 81470M (2011)
- [8] Ghigo, M., Basso, S., Borsa, F., Bavdaz, M., Citterio, O., Civitani, M., et al., "*Development of high angular resolution x-ray telescopes based on slumped glass foils*," Proc. SPIE 8443, 84430R (2012)
- [9] Civitani, M., Basso, S., Citterio, O., Conconi, P., Ghigo, G., Pareschi, G., Proserpio, L., Salmaso, B., Sironi, G., Spiga, D., Tagliaferri, G., Zambra, A., Martelli, F., Parodi, G., Fumi, P., Gallieni, D., Tintori, M., Bavdaz, M., Wille, E., "*Accurate integration of segmented X-ray optics using interfacing ribs*," Optical engineering, 52(9), (2013)
- [10] Salmaso, B., Basso, S., Brizzolari, C., Civitani, M., Ghigo, M., Pareschi, G., Spiga, D., Tagliaferri, G., Vecchi, G., "*Slumped Glass Optics for X-ray telescopes: advances in the hot slumping assisted by pressure*," Proc SPIE 9603, 96030O (2015)
- [11] Salmaso, B., Basso, S., Brizzolari, C., Civitani, M., Ghigo, M., Pareschi, G., Spiga, D., Tagliaferri, G., Vecchi, G., "*Direct hot slumping of thin glass foils for future generation X-ray telescopes: current state of the art and future outlooks*," Proceedings of the 2014 International Conference on Space Optics (2015)

- [12] Salmaso, B., Brizzolari, C., Spiga, D., "A model supporting the use of pressure in the hot slumping of glass substrates for X-ray telescopes," Optics Express, submitted (2016)
- [13] Jimenez-Garate, M. A., Hailey, C. J., Craig, W. W., Christensen, F. E., "Thermal forming of glass microsheets for x-ray telescope mirror segments," Applied Optics 42, 4 (2003)
- [14] Civitani, M., Basso, S., Brizzolari, C., Ghigo, M., Pareschi, G., Salmaso, B., Spiga, D., Tagliaferri, G., Vecchi, G., Breuning, E., Burwitz, V., "Slumped glass optics with interfacing ribs for high angular resolution X-ray astronomy: a progress report," Proc SPIE 9603, 96030P (2015)
- [15] Parodi, G., Martelli, F., Basso, S., Citterio, O., Civitani, M., Conconi, P., Ghigo, M., Pareschi, G., Zambra, A., "Design of the IXO optics based on thin glass plates connected by reinforcing ribs," Proc. SPIE 8147, 81470Q (2011)
- [16] Raimondi, L., Spiga, D., "Mirror for X-ray telescopes: Fresnel diffraction-based computation of point spread functions from metrology," AA 573, A22 (2015)
- [17] Salmaso, B., "Angular resolution improvement of slumped thin glass optics for X-ray telescopes," PhD thesis, Università degli Studi dell'Insubria, (2016)
- [18] Civitani, M.M. Basso, S., Ghigo, M., Salmaso, B., Spiga, D., Vecchi, G., Pareschi, G., "Assemblies of segmented mirrors with interfacing ribs for high angular resolution x-ray telescopes: cold and hot slumped glass optics at work," Proc SPIE 9905, this conference (2016)
- [19] Spiga, D., Barbera, M., Collura, A., Basso, S., Candia, R., Civitani, M., Di Bella, M., Di Cicca, G., Lo Cicero, U., Lullo, G., Pellicciari, C., Riva, M., Salmaso, B., Sciortino, L., Varisco, S., "Manufacturing an active X-ray mirror prototype in thin glass," Journal of Synchrotron Radiation, Vol. 23(1), p. 59-66 (2016)
- [20] Civitani, M., Basso, S., Ghigo, G., Pareschi, G., Salmaso, B., Spiga, D., Tagliaferri, G., Vecchi, G., Burwitz, V., Hartner, G., Menz, B., "X-ray optical units made of glass: achievements and perspectives," Proc. SPIE 9144, 914416 (2014).
- [21] Salmaso, B., Basso, S., Brizzolari, C., Civitani, M.M., Ghigo, M., Pareschi, G., Spiga, D., Tagliaferri, G., Vecchi, G., "Production of thin glass mirrors by hot slumping for X-ray telescopes: present process and ongoing development," Proc SPIE 9151, 91512W (2014)
- [22] Döhring, T., et al., "Forming mandrels for X-ray telescopes made of modified Zerodur," Proc. SPIE 5168, (2004)
- [23] Egle, W., et al., "Figuring, polishing, metrology and performance-analyses of Wolter type I forming mandrels for the Constellation-X mirror development," Proc. SPIE 5488, (2004)
- [24] Civitani, M.M., Ghigo, M., Citterio, O., Conconi, P., Spiga, D., Pareschi, G., Proserpio, L., "3D characterization of thin glass x-ray mirrors via optical profilometry," Proc. SPIE 7803, 78030L (2010)